Adaptive Transparent Impedance Reflecting Teleoperation

K. Hashtrudi–Zaad and S. E. Salcudean *

Dept. of Electrical Engineering

University of British Columbia

Vancouver, BC, V6T 1Z4, Canada

keyvanh@ee.ubc.ca, tims@ee.ubc.ca

Abstract

To achieve transparency for teleoperation in unknown or time varying environments, a class of indirect adaptive bilateral control schemes is developed based on the Slotine and Li "composite adaptive control" schemes and the "impedance bilateral control" architecture presented by Hannaford. The proposed controllers need master and slave position, velocity and acceleration measurements and require no force sensing. Numerical simulations are worked out to demonstrate the transparency and robustness of the controllers to time delay.

1 Introduction

Teleoperation systems have been employed since the pioneering work of Goertz [1] to enable an operator to manipulate dangerous, remote or delicate tasks via a master–slave manipulator with better safety, at lower cost, and even with better accuracy [2].

Besides stability which is the fundamental requirement for every control system, the concept of *telepresence* or *to feel as if operating the task directly*, has been given lots of attention in the past decade [3, 4, 5, 6, 7, 8]. In order to achieve a high degree of telepresence or *transparency* to perform tasks with more accuracy and safety, several bilateral control architectures have been proposed [3, 5, 6, 7, 8, 9, 10]. Lawrence [5], Yokokohji *et.al.* [7] and Salcudean *et.al.* [11] have proposed four–channel architectures that use force and position information from master to slave and vice–versa. Lawrence [5] showed that such architecture is required when linear time–invariant controllers are used.

Niemeyer *et.al* [12] have suggested hybrid control by employing the Slotine and Li (SL) adaptive control scheme for the slave free motion control and stiffness control, emulating a virtual spring, for force control.

However, the need for stability robustness to noise, disturbances and time delays for teleoperation controllers limits performance severely, especially when substantial motion scaling between master and slave is involved [4, 13]. This problem is more significant for operations on unknown environments with large variations in their impedance parameters, such as hitting a hard object (hard contact) [10].

As a potential remedy to this problem, this paper proposes a class of indirect adaptive bilateral control schemes based on the SL *composite adaptive control* schemes [14, 15, 16] and the *impedance bilateral control* architecture proposed by Hannaford [3]. The adaptive schemes use master and slave position, velocity and acceleration measurements to estimate the environment impedance. The estimates are utilized in the slave motion tracking controller and are also fed back to the master controller to provide position and force tracking performance, respectively, *i.e.* to achieve transparency. The ability of the proposed controllers to achieve a high degree of transparency and to resist time delays is demonstrated by simulation results.

Compared to the fixed *transparency optimized* four–channel design in [5], this adaptive methodology does not require force sensing. Instead, it obtains the contact information through the estimate of the environment impedance. Also, compared to the controller presented in [12], the proposed controllers in this paper are designed for transparency. Since the model of the environment is integrated with that of the slave and the estimate of the environment impedance is used to produce force feedback, there is no need to distinguish between slave position control and force control as suggested in [12].

The paper is organized as follows: in Section 2, the SL composite adaptive control scheme for constrained manipulators is formulated. Using the formalism from [5], the adaptive transparent impedance–reflecting teleoperation control is proposed in Section 3. Section 4 presents the simulation results and Section 5 draws conclusions and presents plans for future work.

2 Composite Adaptive Control Strategy for Constrained Manipulators

Consider a robot pushing against an environment with force f as shown in Figure 1. The robot and the environment are modeled by linear time–invariant mass–damper and mass–damper–spring systems with
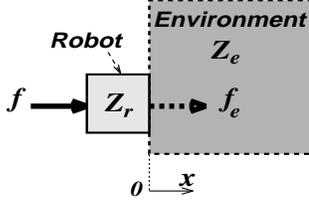
Figure 1: The system of a robot Z_r in contact with an environment Z_e.

impedances $Z_r := m_r s + b_r$ and $Z_e := m_e s + b_e + \frac{k_e}{s}$, respectively, with m_e, b_e, k_e unknown. Then,

$$
\begin{aligned}
f &= m_r \ddot{x} + b_r \dot{x} + f_e \\
&= (m_r + m_e)\ddot{x} + (b_r + b_e)\dot{x} + k_e x \qquad (1) \\
&= Y_{(\ddot{x}, \dot{x}, x)} a \qquad , \qquad (2)
\end{aligned}
$$

where $f_e := m_e \ddot{x} + b_e \dot{x} + k_e x$ is the force exerted on the environment, $Y_{(\ddot{x}, \dot{x}, x)} := [\ddot{x} \ \dot{x} \ x]$, $a := [m_t \ b_t \ k_e]^T$, $m_t := m_r + m_e$ and $b_t := b_r + b_e$.

To control the position of the robot end-effector x to track a desired trajectory x_d and to identify these parameters, the SL composite adaptive control schemes [14, 15, 16] are utilized. The adaptive control law [17] tailored for (2) is

$$
f = Y_{(\ddot{x}_r, \dot{x}_r, x)} \hat{a} - k_v (\dot{x} - \dot{x}_r) \qquad , \qquad (3)
$$

where $\hat{a} := [\hat{m}_t \ \hat{b}_t \ \hat{k}_e]^T = [\hat{m}_e + m_s \ \hat{b}_e + b_s \ \hat{k}_e]^T$, $\dot{x}_r := \dot{x}_d - k_d(x - x_d)$, $\ddot{x}_r = \ddot{x}_d - k_d(\dot{x} - \dot{x}_d)$, $Y_{(\ddot{x}_r, \dot{x}_r, x)} := [\ddot{x}_r \ \dot{x}_r \ x]$, $k_v > 0, k_d > 0$, $x_d = x_d(t)$ is a twice differentiable desired trajectory and $\hat{m}_e, \hat{m}_t, \hat{b}_e, \hat{b}_t$ and $\hat{k}_e$ are estimates of m_e, m_t, b_e, b_t and k_e, respectively[1]. The parameter estimation update law uses both the filtered tracking error $e_r := \dot{x} - \dot{x}_r$, which is a measure of tracking accuracy, and the prediction error of the filtered force $e_w := Y_w \hat{a} - f_w$, and is given by

$$
\dot{\hat{a}}(t) = -P(t)[Y_{(\ddot{x}_r, \dot{x}_r, x)}^T e_r + Y_w^T e_w] \qquad , \qquad (4)
$$

where $P(t)$ is the estimator gain matrix, $Y_w := Y_{(\ddot{x}, \dot{x}, x)} \cdot w(s)$, $f_w := f \cdot w(s)$ and the operator $(\cdot)$ denotes the process of passing the precedent signal, e.g. f, through a strictly stable and proper linear filter with transfer function $w(s)$. The main reason behind using this filter is to avoid acceleration measurement, eg. if $w(s) = \frac{\alpha}{s+\alpha}, \alpha > 0$, then $Y_w = [\alpha(\dot{x} - \dot{x} \cdot w(s)) \ \dot{x} \cdot w(s) \ x \cdot w(s)]$. In addition, by designing the filter $w(s)$ such that its cutoff frequency lies between the system bandwidth and the noise frequency, it is possible to attenuate the degrading effects of the input and measurement noise on the system performance. By virtue of the composite nature of the update law (4) in extracting information from both the prediction and tracking errors for parameter estimation, the adaptive controller (3)–(4), unlike the original SL controller [18, 19], tends to push both e_r and e_w

---

[1] In the literature, $\dot{x}_r$ is called the *reference velocity*.

---

to zero resulting in not only trajectory tracking, but also good parameter convergence. Several composite adaptive controllers emerge from (3)–(4) based on the method by which the gain matrix $P(t)$ is computed [14, 15, 16].

If $P(t) = P_0 > 0$, then the controller is called *Constant Gain* (CG) or *Gradient* composite adaptive controller [15, 16]. Since P is constant, the CG controller works well for systems with abrupt changes in the payload, e.g. for intermittent or hard contact. For this scheme, the trajectory error $e_x := x_d - x$ and e_w globally converge to zero as long as $Y_d := Y_{(\ddot{x}_d, \dot{x}_d, x_d)}$ is bounded. If Y_d is persistently exciting (P.E.), then asymptotic convergence of the parameter estimates to their true values is also guaranteed [15, 16].

If $P(t)$ is updated according to

$$
\dot{P}(t) = \lambda(t) P(t) - P(t) Y_w^T Y_w P(t) \qquad (5)
$$

$$
\lambda(t) = \lambda_0 \left(1 - \frac{\| P(t) \|}{k_0}\right) \qquad , \qquad (6)
$$

where $\lambda_0 > 0$ is the maximum forgetting rate, k_0 is the prespecified upper bound on $\| P(t) \|$ and $0 < P(0) < k_0 I_{3 \times 3}$, then (3)–(6) is called *Bounded–Gain–Forgetting* (BGF) composite adaptive controller [15, 16]. For the update law (5)–(6), it can be shown that for all $t \geq 0, \lambda(t) \geq 0$ and $P(t) \leq k_0 I_{3 \times 3}$. If Y_d is bounded, then e_x and e_w are globally asymptotically convergent to zero. Also if Y_d is P.E., then $\lambda(t)$ and $P(t)$ are bounded away from zero and e_x and $\tilde{a} := \hat{a} - a$ globally exponentially converge to zero [15, 16]. This type of controller suits systems with smoothly time varying parameters. Also, it is more robust to noise and disturbances than the CG scheme.

To avoid parameter drift caused by disturbances which may lead the system to instability, dead–zone [16] or σ–modification [20] techniques can be applied to the parameter adaptation law (5).

In the next section, the SL composite control strategies are employed at the slave side to achieve adaptive transparency in a teleoperation system.

3 Adaptive Transparency

In this section, the application of the SL composite adaptive control schemes to obtain a transparent teleoperation system is considered. In this case $x := x_e$, the slave position, and $x_d := x_h$, the master position command sent from master as shown in Figure 2. As
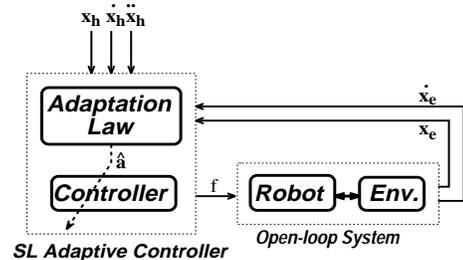

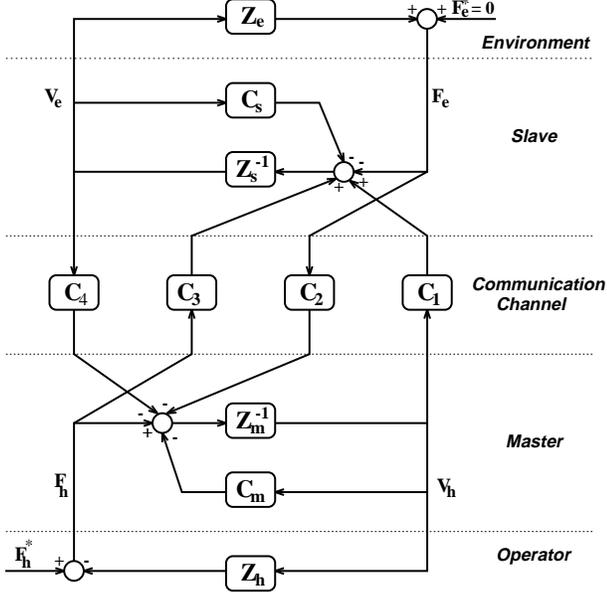Figure 2: SL adaptive controller at the slave side.

Figure 3: General block diagram of a bilaterally controlled teleoperation system (after Lawrence [5]).

a result, $\dot{x}_r = \dot{x}_h - k_d(x_e - x_h)$ and the control and adaptation laws for this system are governed by (3)–(6) with Z_r being replaced by $Z_s := m_s s + b_s$, the impedance of the slave manipulator. As it is clear from Figure 2, $x_e, \dot{x}_e, x_h, \dot{x}_h$ and $\ddot{x}_h$ measurements are needed to construct the slave controller.

So far the control of the slave, regardless of the role of the master and the operator in the control loop has been studied. Next, the control of the master is addressed. Consider the general block diagram of a teleoperation system presented in Figure 3, where $Z_h := m_h s + b_h + \frac{k_h}{s}$ and $Z_m := m_m s + b_m$ represent the impedances of the operator and master, respectively. C_1, C_2, C_3, C_4, C_m and C_s provide feedforward and feedback signals to control the system bilaterally. V_h, V_e are the velocities of the operator's hand and of the slave end–effector and $F_h^\star, F_h, F_e, F_e^\star$ are the force (control) generated by the operator, the force applied by the operator to the master, the force exerted by slave to the environment and the exogenous force generated at the environment, respectively. Since no force measurement is provided, $C_2 = C_3 = 0$. The dynamic equations for this system are

$$F_h^\star = Z_h V_h + F_h \qquad (7)$$
$$F_h = (C_m V_h + C_4 V_e) + Z_m V_h \qquad (8)$$
$$F_e = F_e^\star (= 0) + Z_e V_e \qquad (9)$$
$$F_e = C_1 V_h - C_s V_e - Z_s V_e . \qquad (10)$$

Next, C_1 and C_s are found when the adaptive control strategy is utilized at the slave side and then C_m and C_4 are designed to achieve transparency. Some abuse of notation is used in the sequel in treating the estimates $\hat{m}_t, \hat{b}_t, \hat{k}_e$ as constants so as to be able to show

the dynamical equations in algebraic form (Laplace). As a result of this convention, (3) becomes

$$F = (\hat{m}_t s + (\hat{m}_t k_d + \hat{b}_t + k_v) + \frac{k_d(\hat{b}_t + k_v)}{s}) V_h$$
$$- ((\hat{m}_t k_d + k_v) + \frac{k_d(\hat{b}_t + k_v) - \hat{k}_e}{s}) V_e . \quad (11)$$

With F applied to the slave, C_1 and C_s are identified as the coefficient of V_h and $-V_e$, respectively, that is

$$C_1 = \hat{m}_t s + \hat{b}_t + \hat{C} \qquad (12)$$
$$C_s = \hat{C} - \frac{\hat{k}_e}{s} \qquad (13)$$

where $\hat{C} := \hat{m}_t k_d + k_v + \frac{k_d(\hat{b}_t + k_v)}{s}$. C_4 and C_m are designed to achieve transparency, i.e., a match of the transmitted impedance $Z_t := \frac{F_h}{V_h}$ to the environment impedance Z_e [5, 6]. For the general system of Figure 3, Z_t is computed according to [5]

$$Z_t = \frac{[(Z_m + C_m)(Z_s + C_s) + C_1 C_4] + Z_e(Z_m + C_m + C_1 C_2)}{(Z_s + C_s - C_3 C_4) + Z_e(1 - C_2 C_3)} .$$
$$(14)$$

By substituting for $C_1, C_2, C_3, C_s, Z_m, Z_e$ into (14),

$$Z_t = Z_m + C_m + \frac{(\hat{m}_t s + \hat{b}_t + \hat{C})}{(m_t s + b_t + \hat{C}) + (\frac{k_e - \hat{k}_e}{s})} C_4 \quad (15)$$

is obtained. If $\hat{m}_t, \hat{b}_t$ and $\hat{k}_e$ converge to their true values, then eventually $Z_t \to Z_m + C_m + C_4$. By choosing C_m and C_4 such that $C_m + C_4 = \hat{Z}_e - Z_m$, where $\hat{Z}_e := \hat{m}_e s + \hat{b}_e + \frac{\hat{k}_e}{s}$ and $\hat{m}_e := \hat{m}_t - m_s, \hat{b}_e := \hat{b}_t - b_s$, in the ideal case $Z_t \to \hat{Z}_e \to Z_e$, i.e. the "certainty equivalent" controller will be transparent. Depending on whether $C_m = \hat{Z}_e, C_4 = -Z_m$ or $C_m = -Z_m, C_4 = \hat{Z}_e$, **Type 1** or **Type 2** master controllers are generated, respectively. Type 1 and 2 controllers are special cases of the general block diagram of the closed–loop system shown in Figure 4, where communication time delays are also included. The Type 2 controller, corresponding to cancellation of the master dynamics and employing $\hat{Z}_e$ in the feedback path, has the advantage of avoiding the need to measure $\ddot{x}_e$ when the environment is only modeled as a spring. However, as the simulation results will show in the next section, the Type 1 master controller that uses the environment impedance estimate in the local master controller is more robust to communication time delays and realizes better transparency. This may be explained by noticing that in Type 1, both the estimation dynamic lag and the communication channel delay add up to impose a large delay on V_e, whereas for the other case V_e is delayed only by the communication channel and the estimation lag is modulated on V_h, instead. The stability properties of the proposed schemes are currently under investigation. Since the
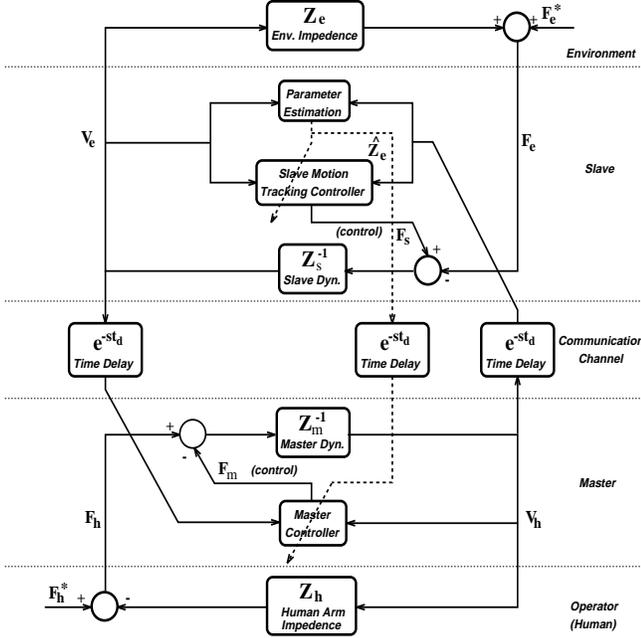
Figure 4: Application of adaptive control to achieve transparency.

Figure 5: Continuous contact simulations: BGF1, no time delay. Notation: keh:=$\hat{k}_e$, beh:=$\hat{b}_e$, meh:=$\hat{m}_e$ and fhs:=$f_h^\star$.

stability results of the SL composite adaptive schemes in Section 2 hinge upon the boundedness of Y_d, therefore once Y_d, which in our case depends on the hand trajectory $x_d = x_h$, is shown to be bounded, the position and force tracking proof follows easily.

In the next section, two sets of simulations are described for a linear model of a teleoperation system using both types of master controllers.

4   Numerical Simulations

Consider the system of Figure 4 with $Z_m = Z_s = 0.7s$ (Ns/m), $Z_h = 0.5s + 70 + \frac{2000}{s}$ (Ns/m), $\hat{Z}_e(0) = 0$ and $f_h^\star$, the operator's hand force, as the input. Assuming the system to be initially at rest and choosing $k_d = k_v = 120, P(0) = diag(0.02, 150, 30000), w(s) = \frac{100}{s+100}, \lambda_0 = 1, k_0 = 40000$ and $f_h^\star = 600(1 - cos(\pi t)) + 150 sin(\frac{\pi}{2}t)$ (N), the following set of simulations were carried out using the Simulink™ simulation package with the Runge–Kutta 45 integration algorithm and step size $1 - 2.5$ (ms):

4.1   Continuous Contact Simulations

The robot is touching the surface of a fairly hard object characterized by $m_e = 1$ (kg), $b_e = 100$ (Ns/m), $k_e = 10000$ (N/m). The force input $f_h^\star$ is applied at the master side to make the slave press against the object without losing the contact. Since there is no loss of contact, the BGF adaptive controller is used at the slave side.

The results of applying the BGF1 bilateral controller, corresponding to utilizing the Type 1 master controller and the BGF slave adaptive controller, are shown in Figure 5. The estimate of the stiffness, which
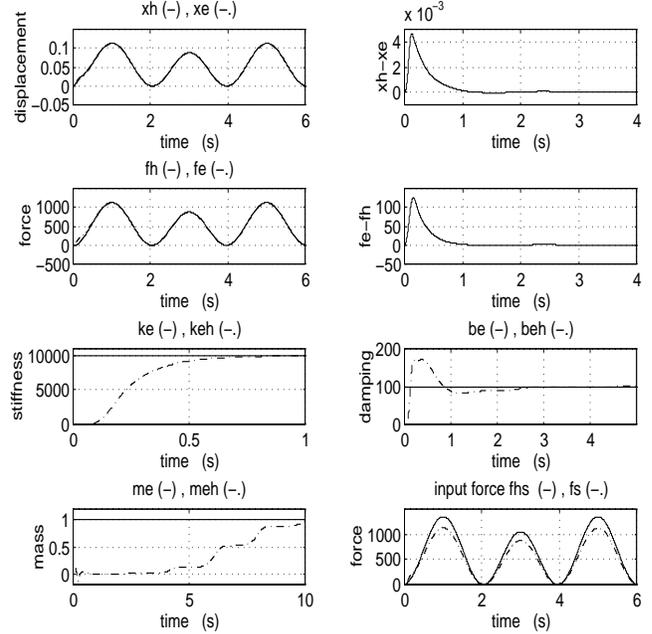
is the dominant part of Z_e at low frequencies, reaches 80% of its final value in 0.4 (s). The force and position tracking performances and, consequently, transparency of the system is satisfactory.

To make a comparison, the tracking error results derived from utilizing BGF1 and BGF2 (Type 2 at master and BGF at slave) are shown in Figure 6. It is clear that BGF1 shows a better force tracking transient and steady state response.

In the presence of time delay, unlike BGF2 that leads to instability even with a 10 (ms) delay, BGF1 performs robustly for $t_d = 100$ (ms), as shown in Figure 7. Also, although with 300 (ms) time delay the force tracking performance degrades significantly, the closed–loop system still remains stable[2].

4.2   Intermittent Contact Simulations

The slave starts at $x_e = 0$ moving towards the same object located at $x_{e0} = 20$ (cm). About 1.5 (s) after the contact, $x_e < x_{e0}$ and the slave moves away from the object until it changes its direction again and moves towards the object. This pattern is followed repeatedly. Similarly to the continuous contact simulations, both Type 1 and 2 controllers are employed at the master side. However, instead of BGF, CG adaptive control has been utilized at the slave side, leading to CG1 and CG2 bilateral master–slave controllers. The results of using CG1 are illustrated in Figure 8. Note that after contact, $\hat{k}_e$ does

---

[2]Due to lack of space, the results of the simulations with $t_d = 300$ (ms) are not shown.
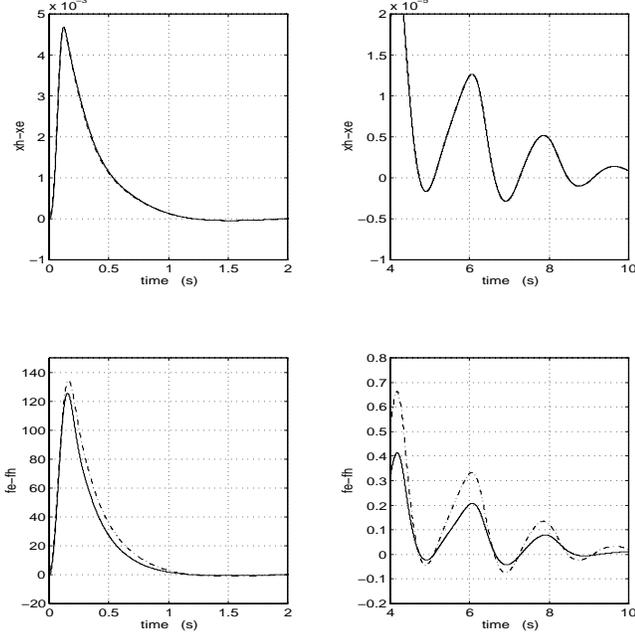
Figure 6: Continuous contact simulations: BGF1 (–), BGF2 (-.), no time delay.

Figure 7: Continuous contact simulations: BGF1, with time delay, $t_d = 100$ (ms). Notation: keh:=$\hat{k}_e$, beh:=$\hat{b}_e$, meh:=$\hat{m}_e$ and fhs:=$f_h^\star$.

not converge to the stiffness of the object which is 10000 (N/m). This is because the controller tends to make the prediction error $e_p := Y_{(\ddot{x}_e, \dot{x}_e, x_e)}\hat{a} - f = (\hat{m}_e - m_e)\ddot{x}_e + (\hat{b}_e - b_e)\dot{x}_e + (\hat{k}_e - k_e)x_e - f_e^\star$ converge to zero in steady state and in this case $f_e^\star = -k_e x_{e0} \neq 0$ for $x_e > x_{e0}$. Therefore

$$e_p = \begin{cases} \hat{m}_e \ddot{x}_e + \hat{b}_e \dot{x}_e + \hat{k}_e x_e & \text{if } x_e \leq x_{e0} \; (= 0.2) \\ (\hat{m}_e - m_e)\ddot{x}_e + (\hat{b}_e - b_e)\dot{x}_e + (\hat{k}_e - k_e)x_e \\ + k_e x_{e0} & \text{otherwise} \end{cases}$$

and by assuming $f_h^\star$ to be rich enough, in steady state, $\hat{k}_e \to k_{av}$, where k_{av} is defined as

$$k_{av} := \begin{cases} 0 & \text{if } x_e \leq x_{e0} \; (= 0.2) \\ k_e - \frac{k_e}{x_e} x_{e0} = 10000 - \frac{2000}{x_e} & \text{otherwise} \end{cases}$$

and may be interpreted as the *average of the environment stiffness over the total slave displacement*. Further simulation results show that, in general, when the environment stiffness distribution is not homogeneous as shown in Figure 9, $\hat{k}_e \to k_{av}$ where

$$k_{av} := \begin{cases} k_{e1} & \text{if } x_e \leq x_{e0} \\ k_{e2} + \frac{(k_{e1} - k_{e2})}{x_e} x_{e0} & \text{otherwise .} \end{cases}$$

The simulation results of using CG1 with time delays are not satisfactory and the system goes unstable for $t_d > 5$ (ms). Also, the simulations for CG2 results in instability.

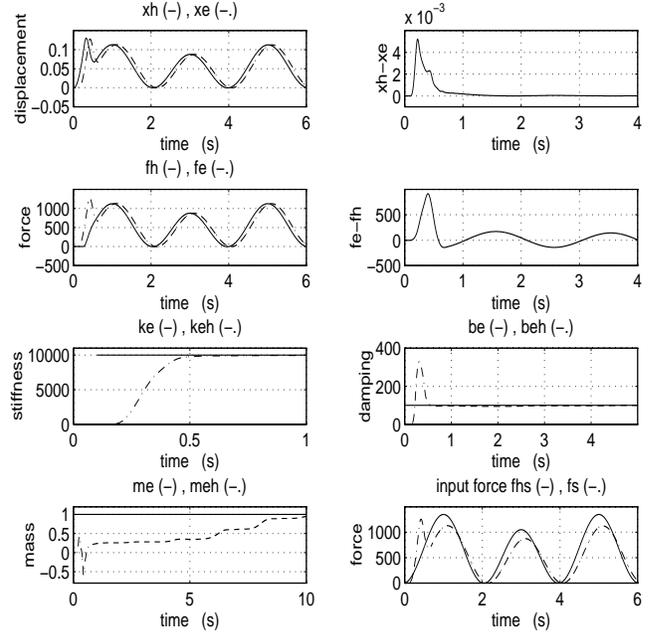In practice, the slave robot may chatter on contact with a stiff object and the estimator may not converge.

As a result the operator may feel the mean value of the contact and non–contact (free motion) environment impedances, *i.e.*, a filtered environment. To solve this problem the authors are developing structurally modified parameter and gain update laws with faster rate of convergence.

5 Conclusions

To maintain stability and transparency for teleoperation in unknown and time varying environments, a class of adaptive transparent impedance reflecting teleoperation control schemes has been developed.

Under simplifying assumptions and without force sensing, the proposed adaptive control strategies, one involving parameter estimates in the master local loop (Type 1) and the other in the feedback path (Type 2), provide *certainty equivalent* transparency. The simulation results are promising and show that Type 1 performs more robustly to time delays and may achieve a better transparency than Type 2 for continuous contact applications. It was also found that Type 1 performs well for intermittent contact applications without time delays while Type 2 goes unstable. The stability analysis of these schemes is currently under investigation.

Future work should include the implementation of the adaptive strategies on teleoperation testbeds such as a mini–excavator or a motion scaling system used for microsurgery experiments. Also, the force sensing information may be used to provide faster adaptation and to remove the need for acceleration signals to make the controllers more practical.
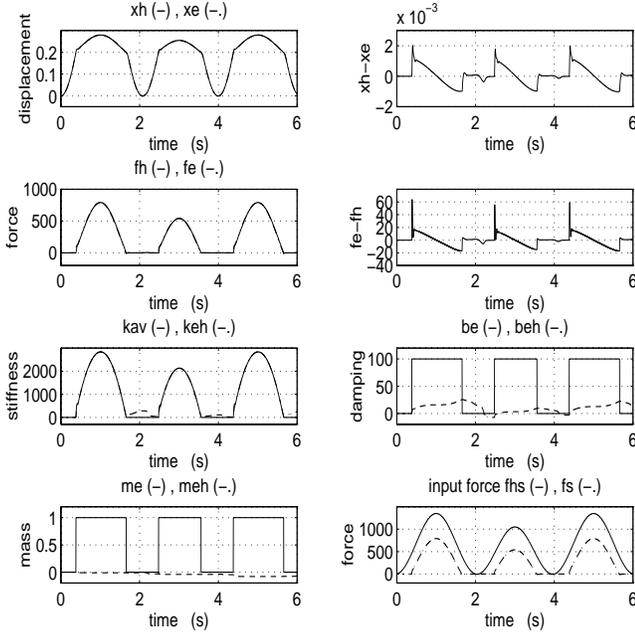
Figure 8: Intermittent contact simulations: CG1, no time delay. Notation: keh:=$\hat{k}_e$, beh:=$\hat{b}_e$, meh:=$\hat{m}_e$ and fhs:=$f_h^\star$.
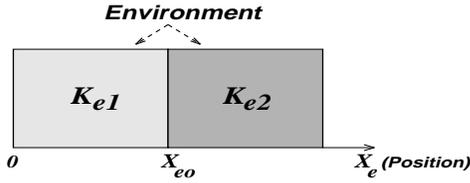

Figure 9: Schematic of the environment stiffness distribution.

References

[1] Goertz R.C.,"Manipulator Systems Development at ANL," *Proceedings of the 12th Conference on Remote Systems Technology*, American Nuclear Society, pp. 117–136, 1954.

[2] Sheridan T.B.,"Telerobotics," *Automatica*, Vol. 25, No. 4, pp. 487–507, 1989.

[3] Hannaford B.,"Design Framework for Teleoperators with Kinesthetic Feedback," *IEEE Trans. Auto. Cont.*, Vol. 5, No. 4, pp. 426–434, 1989.

[4] Hannaford B.,"Stability and Performance Tradeoffs in Bilateral Telemanipulation," *Proc. IEEE Int. Conf. Rob. & Auto.*, pp. 1764–1767, 1989.

[5] Lawrence D.A.,"Designing Teleoperator Architectures for Transparency," *Proc. IEEE Int. Conf. Rob. & Auto.*, pp. 1406–1411, Nice, France, 1992.

[6] Raju G.J., Verghese G.C. and Sheridan T.B.,"Design Issues in 2–port Network Models of Bilateral Remote Manipulation," *Proc. IEEE Int. Conf. Rob. & Auto.*, pp. 1316–1321, 1989.

[7] Yokokohji Y. and Yoshikawa Tsuneo,"Bilateral Control of Master–slave Manipulators for Ideal Kinesthetic Coupling: Formulation and Experiment," *Proc. IEEE Int. Conf. Rob. & Auto.*, pp. 849–858, Nice, France, 1992.

[8] Zhu M. and Salcudean S.E.,"Achieving Transparency for Teleoperator Systems Under Position and Rate Control," *Proc. IEEE/RSJ Int. Conf. Intelligent Robots & Systems*, pp. 7–12, Pittsburgh, P.A., 1995.

[9] Brooks T.L.,"Telerobotic Response Requirements," *Proc. IEEE Int. Conf. Sys., Man, & Cyber.*, pp. 113–120, 1990.

[10] Hannaford B. and Anderson R.,"Experimental and Simulation Studies of Hard Contact in Force Reflecting Teleoperation," *Proc. IEEE Int. Conf. Rob. & Auto.*, pp. 584–589, 1988.

[11] Salcudean S.E., Wong M.W. and Hollis R.L.,"A Force Reflecting Teleoperation System with Magnetically Levitated Master and Wrist," *Proc. IEEE Int. Conf. Rob. & Auto.*, Nice, France, 1992.

[12] Niemeyer G. and Slotine J.J.E.,"Stable Adaptive Teleoperation," *IEEE Jour. Oceanic Engineering*, Vol. 16, No. 1, pp. 152–162, 1991.

[13] Salcudean S.E., Yan J., Hu J. and Loewen P.,"Performance Tradeoffs in Optimization-based Teleoperation Controller Design with Applications to Microsurgery Experiments," *Proc. Int. Mechanical Engineering Congress & Exposition*, DSC–Vol. 57–2, pp. 631–640, Nov. 1995.

[14] Slotine J.J.E. and Li W.,"Adaptive Robot Control: A New Perspective," *Proc. IEEE Int. Conf. Dec. & Cont.*, pp. 192–198, Los Angeles, CA, 1987.

[15] Slotine J.J.E. and Li W.,"Composite Adaptive Control of Robot Manipulators," *Automatica*, Vol. 25, N0. 4, pp. 509–519, 1989.

[16] Slotine J.J.E. and Li W.,"Applied Nonlinear Control," Prentice–Hall, 1991.

[17] Slotine J.J.E. and Li W.,"Adaptive Strategies in Constrained Manipulation," *Proc. IEEE Int. Conf. Rob. & Auto.*, pp. 595–601, 1987.

[18] Slotine J.J.E. and Li W.,"On the Adaptive Control of Robot Manipulators," *Int. Jour. Rob. Res.*, Vol. 6, No. 3, pp. 49–59, 1987.

[19] Slotine J.J.E. and Li W.,"Theoretical Issues in Adaptive Manipulator Control," *Proc. Fifth Yale Workshop on Applications of Adaptive Systems Theory*, pp. 252–258, 1987.

[20] Reed J.S. and Ioannou P.A.,"Instability Analysis and Robust Adaptive Control of Robotic Manipulators," *Proc. IEEE Int. Conf. Dec. & Cont.*, pp. 1607–1612, 1988.